International Journal of Dynamics and Control
https://doi.org/10.1007/s40435-018-0467-2

Experimental study on a nonlinear observer application for a very flexible parallel robot

Fatemeh Ansarieshlaghi[1] · **Peter Eberhard**[1]

Received: 30 May 2018 / Revised: 19 July 2018 / Accepted: 10 August 2018

Abstract
A flexible robot in lambda configuration has been modeled and built in hardware. This flexible robot includes some passive joints and flexible bodies and is an underactuated system. In order to control a very flexible underactuated system, using all states of the modeled nonlinear system is advantageous. Since there is no direct measurement of the end-effector positions and all modeled system states available, a nonlinear observer to estimate the states, the rigid motion of the passive joints and the elastic deformation of the flexible bodies, is designed based on the high gain observer method and experimentally tested on the lambda robot. Using the observed results from the nonlinear observer, the model of the robot used for control is improved so that the end-effector tracking error is drastically decreased. Based on the improved model, an updated nonlinear observer is redesigned and implemented on the lambda robot. The experimental results show that the end-effector positions and the states can be estimated with high accuracy in real-time even for the highly flexible parallel robot.

Keywords Flexible parallel robot · Nonlinear observer · Multibody dynamics · State estimation

1 Introduction

Manipulator designs often intend to provide maximized stiffness to avoid undesired deformations and vibrations. This results in high accuracy in the end-effector trajectory tracking, while it usually includes a drastic mass increase, a poor weight-to-payload ratio, and high energy consumption. In contrast, light weight manipulators attract a lot of research interest because of their complementing advantages. The advantages of light weight robots include low energy usage, less mass, and often high working speeds. However, due to the light weight design, the bodies have a significant flexibility which yields undesired deformations and vibrations. Therefore, the manipulators are modeled as flexible multibody systems and the flexibilities must be taken into account in the control design. Flexible manipulators are typical examples of underactuated multibody systems since they generally have fewer control inputs than degrees of freedom for rigid body motion and deformations. In order to obtain a good performance in the end-effector trajectory tracking of a flexible manipulator, an accurate and efficient nonlinear control is necessary. Therefore, to control the flexible multibody system with high performance, using accurate models is required. Hence, the flexibility of the links shall be considered in the model. The difficulty of designing a nonlinear controller with high performance for high flexibility is increased when the controller does not have access to direct measurement of the end-effector and all the system states. To overcome this problem, the design of a nonlinear observer to estimate the position of end-effector and the system states is necessary.

Much research has been done on the modeling and dynamic analysis of flexible multibody systems. The modeling of flexible multibody robots is separated into single-link and multi-link flexible manipulators. The single-link flexible manipulator modeling approaches can be categorized, e.g., into assumed mode method, finite element method, lumped parameter models, and other studies based on [1]. Also, the modeling of multi-link flexible manipulators is investigated in many contributions, especially for the modeling of two flexible link manipulators [2], or for more than two flexible links [3–6]. Furthermore, the modeling of rigid-flexible link manipulators has been investigated [7].

✉ Fatemeh Ansarieshlaghi
fatemeh.ansari@itm.uni-stuttgart.de

Peter Eberhard
peter.eberhard@itm.uni-stuttgart.de

[1] Institute of Engineering and Computational Mechanics, Universityof Stuttgart, 70569 Stuttgart, Germany

Published online: 16 August 2018

Observers are widely used in order to estimate the full state of a modeled system, see e.g. for the linear systems [8], for velocity estimation of the rigid joints [9], for state estimation of non-minimum and minimum phase systems [10], and for state estimation under high frequency measurement noise [11,12].

State estimation of a single flexible link manipulator and flexible multibody systems are investigated, e.g. the design of a linear observer for a flexible multibody system without passive joint [3] for observing the measurement noises, simulation of the observer design for a flexible beam [13,14]. So far, experimental research is focused on the observation of a flexible beam to estimate the vibration using a laser displacement sensor [15]. Also, for the flexible lambda robot, a nonlinear state estimation using Unscented Kalman Filter was designed [16] to control the end-effector position based on the rigid model.

Main problems of the flexible-link manipulator control can be categorized into end-effector position control, rest to rest end-effector motion control in fixed time, trajectory tracking in the joint space, and tracking of desired end-effector trajectory in [17]. Model-based control methods often use feedforward controllers and non model-based approaches often use feedback controllers [18]. Controller design and implementation on a single flexible link manipulator in simulation [19] and experiment [20], and control a two-link flexible serial manipulator in simulation [21] are discussed.

In this research, we used the model-based controllers to reach high accuracy and high performance for controlling the end-effector positions and the joints control of a multi-link flexible manipulator. Here, the model-based control is used to solve the inverse dynamics using a two points boundary value problem and finding the desired trajectory. In the feedback controller part, the static controller is used to track the desired trajectories for actuated joints.

The novelty of this work is, that a nonlinear high gain observer for high-speed trajectory tracking of a very flexible parallel robot is designed which only uses the position and the velocity measurement of the prismatic joints and the deformation of the long flexible link to estimate the finite number of elastic, passive states, and end-effector position. The main novelty of this paper is not the theoretical part instead, it is in the experimental part where the high gain observer method is applied for a very complicated flexible system. This system includes a lot of mechanical hardware challenges such as passive joints and very flexible links that are contained in the flexible multibody system of the lambda robot.

This nonlinear observer is simulated and implemented on the lambda robot. Experimental results of the designed observer show that the lambda robot does not behave precisely as the model. Therefore, the model is updated by observing the system behavior and comparing it with the experiment. Using the updated model, the feedforward controller calculates the desired sets for the feedback controller. Measurement results show that the tracking error and oscillation amplitude are drastically decreased for the linear and nonlinear trajectories with high-speed motion. Also, the nonlinear observer based on the improved model estimates the system states and the end-effector position with higher accuracy. Some experimental results verify the precision of the observer to estimate the end-effector positions and the elastic deformations.

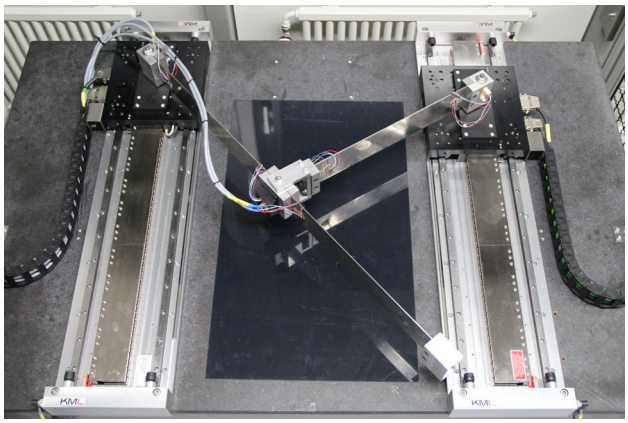

Fig. 1 Mechanical setup of the lambda manipulator

The paper is organized as follows: Sect. 2 is about the robot hardware and Sect. 3 includes the modeling of the flexible parallel manipulator. In Sect. 4, the formulation and design of the nonlinear observer are explained. Section 5 includes control schemes, i.e. the feedforward and feedback control. In Sect. 6, the proposed observer is executed on the hardware and the results are discussed.

2 Flexible parallel lambda robot

A flexible robot in lambda configuration which has been built [22] at the Institute of Engineering and Computational Mechanics of the University of Stuttgart can be seen in Fig. 1.

This robot has highly flexible links. The links of the robot are very flexible and they have high oscillation amplitude compared to the length of the links. The end of the short link is connected in the middle of the long link using rigid bodies. The robot has two prismatic actuators connecting the links to the ground. The links are connected using passive revolute joints to the linear actuators. Another revolute joint is used to connect the short link and the middle of the long link. An additional rigid body is attached to the free end of the long link as an end-effector. The drive positions and velocities are measured with optical encoders. Two full Wheatstone bridge strain gauges are attached to measure the deformation of the flexible long link. These strain gauges are installed at two

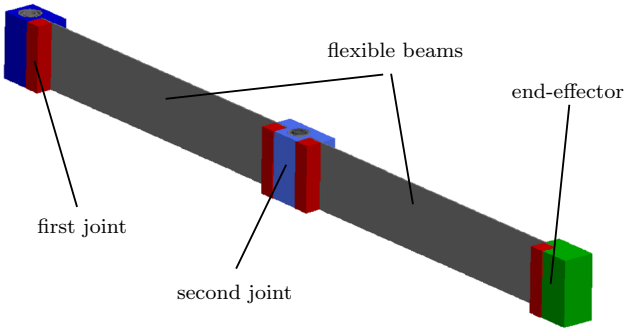

Fig. 2 Flexible long link

sides of the passive joints on the long link can be seen in Fig. 1. This passive joint is used to connect the end of the short link and the middle of the long link.

The online control is done with a *Speedgoat* performance real-time target machine running *Mathworks xPCtarget* kernel, which is called *Simulink* Real-Time since *Matlab R2014a*. In order to do the control and have access to the input, output, safety logic, and controller of the lambda robot and their communication, a graphical user interface is available [23].

3 Flexible multibody modeling

The modeling process can be separated into three major steps. First, the flexible components of the system are modeled with the linear finite element method in the commercial finite element code *ANSYS*. Next, for online control, the degrees of freedom of the flexible bodies shall be decreased. Therefore, model order reduction is utilized [22] using *MatMorembs* [24]. Then, all the rigid and flexible parts are modeled as a multibody system with a kinematic loop using the academic multibody code *Neweul-M*^{2} [25].

The flexible beams, i.e. the thin parts of the long link, are shown in Fig. 2 and are modeled using Timoshenko beam elements. For each beam, one hundred beam elements, that are constrained to the horizontal plane, are used. Additionally, the rigid bodies, e.g. the passive joints and the end-effector, are attached to the flexible segments. So, the defined elastic bodies include two hundred beam elements and some rigid bodies yielding in total to about six hundred degrees of freedom [22]. Also, the movement constraint of the link shall be taken into account. Therefore, two translations for the nodal frame at the first joint and one translation for the second joint are locked. Next, the modal analysis is utilized to determine the natural frequencies and mode shapes of the long link in *ANSYS*. The overall rigid body motion of the long link is described by a nonlinear approach while the small elastic deformation around this guiding motion are modeled as a linear system with some mode shapes.

In the next step, the *ANSYS* output is used for model order reduction in *MatMorembs*. The modal model order reduction method is used to reduce the order of flexible multibody model. The reduced flexible link model is exported to the SID-file format [26].

Finally, the flexible long link, the short link, two linear drivers and three revolute joints are assembled as a flexible multibody system in *Neweul-M*^{2}. The equation of motion with a kinematic loop constraint, using the generalized coordinates $\boldsymbol{q} \in \mathbb{R}^n$ is

$$\boldsymbol{M}(\boldsymbol{q})\ddot{\boldsymbol{q}} + \boldsymbol{k}(\boldsymbol{q}, \dot{\boldsymbol{q}}) = \boldsymbol{g}(\boldsymbol{q}, \dot{\boldsymbol{q}}) + \boldsymbol{B}\boldsymbol{u} + \boldsymbol{C}^{\mathrm{T}}(\boldsymbol{q})\boldsymbol{\lambda}, \tag{1a}$$

$$\boldsymbol{c}(\boldsymbol{q}) = \boldsymbol{0}. \tag{1b}$$

The symmetric, positive definite mass matrix $\boldsymbol{M} \in \mathbb{R}^{n\times n}$ depends on the joint angles and the elastic coordinates. The vector $\boldsymbol{k} \in \mathbb{R}^n$ contains the generalized centrifugal, Coriolis and Euler forces, and $\boldsymbol{g} \in \mathbb{R}^n$ includes the vector of applied forces and inner forces due to the body elasticity. The input matrix $\boldsymbol{B} \in \mathbb{R}^{n\times p}$ maps the input vector $\boldsymbol{u} \in \mathbb{R}^p$ to the system. The constraint equations are defined by $\boldsymbol{c} \in \mathbb{R}^m$. The Jacobian matrix of the constraint $\boldsymbol{C} = \partial\,(\boldsymbol{c}(\boldsymbol{q}))/\partial\boldsymbol{q} \in \mathbb{R}^{m\times n}$ maps the reaction force $\boldsymbol{\lambda} \in \mathbb{R}^m$ due to the kinematic loop. Using QR decomposition of the Jacobian matrix of the constraints, the term $\boldsymbol{C}^T\boldsymbol{\lambda}$ can be removed [5]. The equation of motion can be formulated as

$$\overline{\boldsymbol{M}}(\boldsymbol{q})\ddot{\boldsymbol{q}} + \overline{\boldsymbol{k}}(\dot{\boldsymbol{q}}, \boldsymbol{q}) = \overline{\boldsymbol{g}}(\dot{\boldsymbol{q}}, \boldsymbol{q}) + \overline{\boldsymbol{B}}(\boldsymbol{q})\boldsymbol{u}. \tag{2}$$

The lambda robot model is a strongly nonlinear system. It includes e.g. the coupling of the flexible and rigid bodies which requires a nonlinear description of motion. Nonlinear functions such as sine or cosine of occurring angles, and quadratic functions of the generalized coordinates show up in the formulation. A linearized of the system behavior would only be feasible if only small motions are performed which is certainly not the case here.

Figure 3 shows the flexible parallel lambda robot in *Neweul-M*^{2}. The lambda robot is modeled with ten degrees of freedom $\boldsymbol{q} \in \mathbb{R}^{10}$. The generalized coordinates $\boldsymbol{q} = [\boldsymbol{q}_e, \boldsymbol{q}_r]^T$ include the elastic coordinates of the long link $\boldsymbol{q}_e \in \mathbb{R}^6$ and the rigid degrees of freedom $\boldsymbol{q}_r \in \mathbb{R}^4$. The vector of rigid body coordinates includes two active prismatic joint positions (s_1, s_2) and two passive revolute joint angles (α_1, α_2) which are shown in Fig. 3.

The nonlinear dynamic equation of motion of the lambda robot can be written in state space form as

$$\dot{\boldsymbol{x}} = \boldsymbol{A}\boldsymbol{x} + \boldsymbol{d}(\boldsymbol{x}) + \boldsymbol{H}(\boldsymbol{x})\boldsymbol{u}, \tag{3a}$$

$$\boldsymbol{y} = \boldsymbol{W}\boldsymbol{x}. \tag{3b}$$

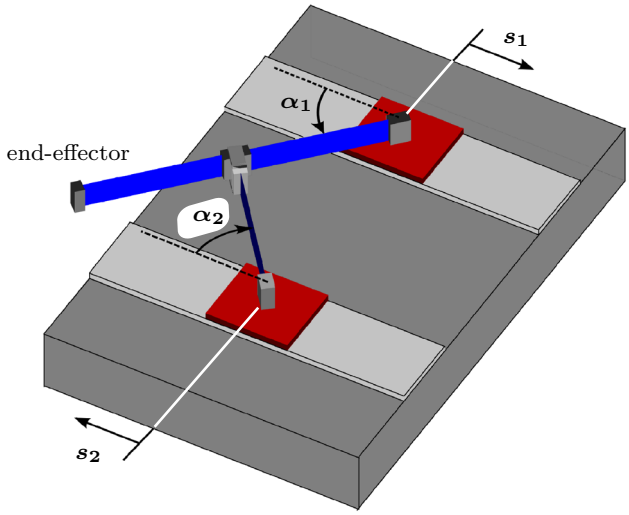

Fig. 3 Flexible parallel lambda robot

Here $\boldsymbol{x} = [\boldsymbol{x}_1, \boldsymbol{x}_2]^T \in \mathbb{R}^{20}$ are the system states, $\boldsymbol{x}_1 = \boldsymbol{q}$ and $\boldsymbol{x}_2 = \dot{\boldsymbol{q}}$, which are the generalized coordinates and derivatives of the generalized coordinates. The constant matrix $\boldsymbol{A} \in \mathbb{R}^{20\times 20}$ is the linear part of the system dynamics, $\boldsymbol{d} \in \mathbb{R}^{20}$ is the nonlinear part of the system dynamics, and $\boldsymbol{H} \in \mathbb{R}^{20\times 2}$ is a nonlinear function depending on the system states which maps the inputs $\boldsymbol{u} \in \mathbb{R}^2$ to the lambda robot. The inputs of the lambda robot are the current of actuators. The flexible robot outputs and the output constant matrix are defined with $\boldsymbol{y} \in \mathbb{R}^5$ and $\boldsymbol{W} \in \mathbb{R}^{20\times 5}$, respectively. The outputs of the lambda robot are the position and the velocity of the prismatic joints and the deformation of the flexible long link.

4 Nonlinear observer

Now, a nonlinear high gain observer for the lambda robot is introduced to estimate the states and the end-effector position. To this end, the dynamics description of the lambda robot in state space form, Eq. (3), can be written as

$$\dot{\boldsymbol{x}} = \boldsymbol{A}\boldsymbol{x} + \boldsymbol{f}(\boldsymbol{x}), \tag{4a}$$

$$\boldsymbol{y} = \boldsymbol{W}\boldsymbol{x}, \tag{4b}$$

where $\boldsymbol{f}(\boldsymbol{x}) \in \mathbb{R}^{20}$ is a nonlinear function

$$\boldsymbol{f}(\boldsymbol{x}) = \boldsymbol{d}(\boldsymbol{x}) + \boldsymbol{H}(\boldsymbol{x})\boldsymbol{u}. \tag{5}$$

State estimation for the system in Eq. (4) is used to design a nonlinear high gain observer based on the methods in [27,28]. The dynamics of the proposed observer is formulated as

$$\dot{\hat{\boldsymbol{x}}} = \boldsymbol{A}\hat{\boldsymbol{x}} + \boldsymbol{f}(\hat{\boldsymbol{x}}) + \boldsymbol{L}(\hat{\boldsymbol{y}} - \boldsymbol{y}), \tag{6a}$$

$$\hat{\boldsymbol{y}} = \boldsymbol{W}\hat{\boldsymbol{x}}, \tag{6b}$$

where $\hat{\boldsymbol{x}}$ and $\hat{\boldsymbol{y}}$ are the estimated states and outputs of the observed system, respectively. Therefore, the observer gain $\boldsymbol{L} \in \mathbb{R}^{20\times 5}$ shall be designed somehow such that the estimated states converge to the real system states. The observation error is different between the estimated and real system states and is calculated by $\boldsymbol{e} = \hat{\boldsymbol{x}} - \boldsymbol{x}$. The dynamics of the estimation error is obtained

$$\dot{\boldsymbol{e}} = (\boldsymbol{A} + \boldsymbol{L}\boldsymbol{W})\boldsymbol{e} + (\boldsymbol{f}(\hat{\boldsymbol{x}}) - \boldsymbol{f}(\boldsymbol{x})). \tag{7}$$

If the nonlinear dynamic error in Eq. (7) converges asymptotically to zero, it can be concluded that the estimated states converge to the real system states. For this purpose, the Lyapunov function and the Lipschitz condition are used. The Lyapunov candidate function is defined as a positive definite function with a unique positive definite matrix $\boldsymbol{P} \in \mathbb{R}^{20\times 20}$

$$V(\boldsymbol{e}) = \boldsymbol{e}^T\boldsymbol{P}\boldsymbol{e}. \tag{8}$$

The derivative of the Lyapunov function is calculated as

$$\begin{aligned}\dot{V}(\boldsymbol{e}) = \boldsymbol{e}^T((\boldsymbol{A} + \boldsymbol{L}\boldsymbol{W})^T\boldsymbol{P} + \boldsymbol{P}(\boldsymbol{A} + \boldsymbol{L}\boldsymbol{W}))\boldsymbol{e} \\ + (\boldsymbol{f}(\hat{\boldsymbol{x}}) - \boldsymbol{f}(\boldsymbol{x}))^T\boldsymbol{P}\boldsymbol{e} + \boldsymbol{e}^T\boldsymbol{P}(\boldsymbol{f}(\hat{\boldsymbol{x}}) - \boldsymbol{f}(\boldsymbol{x})).\end{aligned} \tag{9}$$

The derivative of the Lyapunov function must be negative to ensure that the estimation error converges asymptotically to zero. Towards this goal, an additional constraint is required. The nonlinear function of the lambda robot $\boldsymbol{f}(\boldsymbol{x})$ must satisfy the Lipschitz condition, too. Based on the Lipschitz condition, there exists a constant G such that

$$\|\boldsymbol{f}(\hat{\boldsymbol{x}}_i) - \boldsymbol{f}(\boldsymbol{x}_i)\| \leqslant G\|\hat{\boldsymbol{x}}_i - \boldsymbol{x}_i\|, \quad \forall i = 1, \ldots, 20 \tag{10}$$

for all $\boldsymbol{x}$ and $\hat{\boldsymbol{x}}$. Also, there exists a positive definite matrix $\boldsymbol{Q} \in \mathbb{R}^{20\times 20}$ that is defined from

$$(\boldsymbol{A} + \boldsymbol{L}\boldsymbol{W})^T\boldsymbol{P} + \boldsymbol{P}(\boldsymbol{A} + \boldsymbol{L}\boldsymbol{W}) = -2\boldsymbol{Q}. \tag{11}$$

Therefore, for Eq. (9), the following inequality is valid

$$\begin{aligned}\dot{V}(\boldsymbol{e}) &\leqslant -2\boldsymbol{e}^T\boldsymbol{Q}\boldsymbol{e} + 2G\|\boldsymbol{P}\boldsymbol{e}\|\|\boldsymbol{e}\| \\ &\leqslant (-2\sigma_{\min}(\boldsymbol{Q}) + 2G\sigma_{\max}(\boldsymbol{P}))\|\boldsymbol{e}\|^2.\end{aligned} \tag{12}$$

Here, $\sigma_{\min}(\boldsymbol{Q})$ is the minimum singular value of the matrix $\boldsymbol{Q}$ and $\sigma_{\max}(\boldsymbol{P})$ is the maximum singular value of the matrix $\boldsymbol{P}$. In order to have a negative derivative of the candidate Lyapunov function V, the inequality for the matrices $\boldsymbol{Q}$ and $\boldsymbol{P}$ must be hold

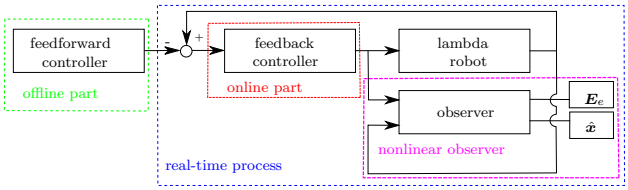

Fig. 4 Control block diagram

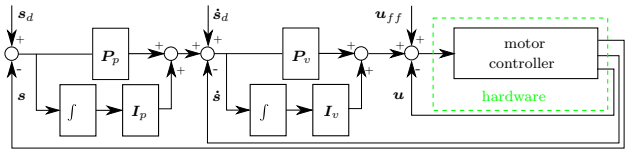

Fig. 5 Feedback control block diagram

$$\frac{\sigma_{\min}(\boldsymbol{Q})}{\sigma_{\max}(\boldsymbol{P})} \leqslant G. \tag{13}$$

The estimated states converge to the real system measurements if all the conditions on the defined matrices $\boldsymbol{L}$, $\boldsymbol{Q}$, and $\boldsymbol{P}$ are satisfied. Figure 4 shows how the observer is included in the real-time process. The values $\hat{\boldsymbol{x}}$ and $\boldsymbol{E}_e$ are outputs of the nonlinear observer, i.e. the estimated states and end-effector positions, respectively.

5 Control schemes

The lambda robot control strategy is separated into feedforward and feedback control parts. In the feedforward control part, the desired trajectories for system states are calculated using a two-point boundary value problem as offline while the flexible multibody system is a non-minimum phase system with internal dynamics. The results of the feedforward part are the desired values for the feedback control part. The feedback controller is executed to minimize the actuator tracking error in real-time.

5.1 Feedforward control part

The feedforward controller is obtained by solving a two-point boundary value problem for the exact model inversion of the complete dynamical model of the multibody system. To force the end-effector to track a trajectory, an additional constraint equation, so-called servo constraint [29], is augmented to the equation of motion (1). The equation of motion with the new servo constraint can be written as

$$\boldsymbol{M}\ddot{\boldsymbol{q}} + \boldsymbol{k}(\dot{\boldsymbol{q}}, \boldsymbol{q}) = \boldsymbol{g}(\dot{\boldsymbol{q}}, \boldsymbol{q}) + \boldsymbol{B}\boldsymbol{u} + \boldsymbol{C}^T\boldsymbol{\lambda}, \tag{14a}$$

$$\boldsymbol{c}(\boldsymbol{q}) = \boldsymbol{0}, \tag{14b}$$

$$\boldsymbol{s}(t, \boldsymbol{q}) = \boldsymbol{0}. \tag{14c}$$

These differential-algebraic equations describe the inverse model of the multibody system with some constraints. The lambda robot has an internal dynamics since it includes passive joints and flexible states as underactuated generalized coordinates. That means that, a part of the dynamics, which includes the passive and flexible states, is not observable. Since the internal dynamics is not solvable for the inverse dynamics, the servo constraint is defined to obtain the desired sets of the generalized coordinates for a certain path. In the end-effector trajectory tracking, the internal dynamics of the flexible multibody system is unstable because the inputs do not have control over them. Therefore, the equation of motion with constraints is required to solve the two-point boundary value problem, which results in bounded interval values for the system inputs and for the minimized coordinates and their time derivatives.

The solution of the boundary value problem is computed in *Matlab* using the solver *bvp5c*. The boundary conditions are calculated in such a way that the solution starts on the unstable manifold and ends on the stable manifold of the internal dynamics. This can be seen from the experimental results of the end-effector vibration in the first milliseconds of trajectories. The set values of the dependent coordinates, the independent coordinates, the inputs of the system, and the Lagrange multipliers are obtained from the constraint equations on the position, velocity, and acceleration level.

5.2 Feedback control part

The desired and measurement values of the position and velocity of the prismatic joints are compared as the input for the online controller. The controller computes the input of the robot in the real-time procedure. Figure 5 shows the online controller procedure of the lambda robot.

The feedback controller part, i.e. the static controller, is included in the PI controller. The constant gains of the feedback controller are selected using Bode plot stability analysis of the prismatic actuators and experimental tuning of these gains.

The motor controller sets the current of the servo drives and the prismatic joint controller that is used to control the position and the velocity of the prismatic actuators of the robot. The matrices $\boldsymbol{P}_p$, $\boldsymbol{P}_v$, $\boldsymbol{I}_p$, and $\boldsymbol{I}_v$ are the constant gain matrices of the feedback controller for the position and velocity control of the prismatic joints. Here, the desired values for the position, the velocity, and the feedforward current of the actuators are referred with $\boldsymbol{s}_d$, $\dot{\boldsymbol{s}}_d$, and $\boldsymbol{u}_{ff}$, respectively. The measurement values $\boldsymbol{s}$, $\dot{\boldsymbol{s}}$, and $\boldsymbol{u}$ are the position, velocity, and current of the drivers.

Fig. 6 Offline image processing result for the recorded movie of end-effector trajectory tracking

6 Experimental results

6.1 Experiment setup

The controller is tested in real-time on the machine with 250 µs sampling time. Therefore, the camera is not applicable for online tracking of the end-effector position and it can be used only for offline validation. To validate the measurement and estimation results for the end-effector position, a camera that is installed above of the lambda robot is used. Two light points are attached on the end-effector and they are tracked using the offline image processing for the recorded movie during the robot motion. Figure 6 shows an offline image processing result of the recorded movie for tracking a line trajectory.

Furthermore, a strain gauge is used to measure the deformation of the flexible long link to estimate the elastic states of the lambda robot. To show the accuracy of the estimation results, the deformation of a strain gauge and the observed deformation for the long link are compared.

6.2 Model improvement

Now, the proposed nonlinear observer based on the model in [23] is utilized to estimate the states of the system. Hence, the computed observation results are compared in Fig. 7 with the measured image processing results of the end-effector position. Although in Fig. 7b the estimated elastic coordinates results are closer to the strain gauge measurements, the estimated end-effector position in Fig. 7a is not really close to the measured validation results.

As a result, the model of the robot that transfers the generated coordinates to the end-effector is not yet sufficiently accurate. Also, the experimental investigation of the lambda robot shows oscillation frequencies of the model and the real system are different. Therefore, to solve this problem, the model and the real system behavior are carefully investigated. For this, the model is updated by observing the computed system behavior and comparing it with the experiment. Consequently, the height and the stiffness of the flexible beams are decreased. Additionally, the flexibility of the short link is taken into account for modeling of the lambda robot. The natural frequencies of the improved model and the model without improvement for the links are compared in Table 1. The model without improvement is called model-1 and the improved model is called model-2.

Table 1 that shows that the eigen frequencies of model-2 are smaller than of model-1. That means that the flexibility of the long link in model-2 is higher than that of model-

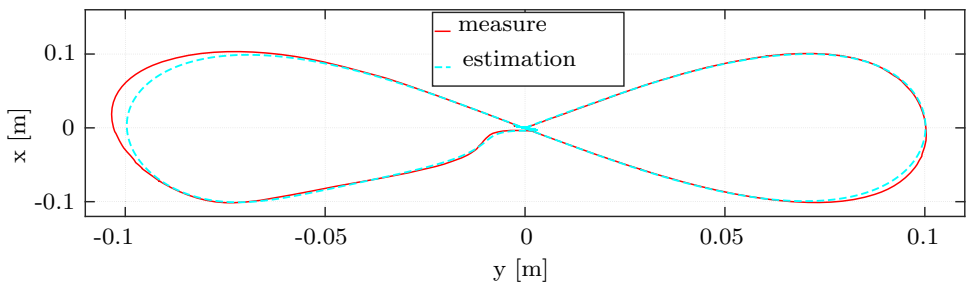

(a) End-effector position

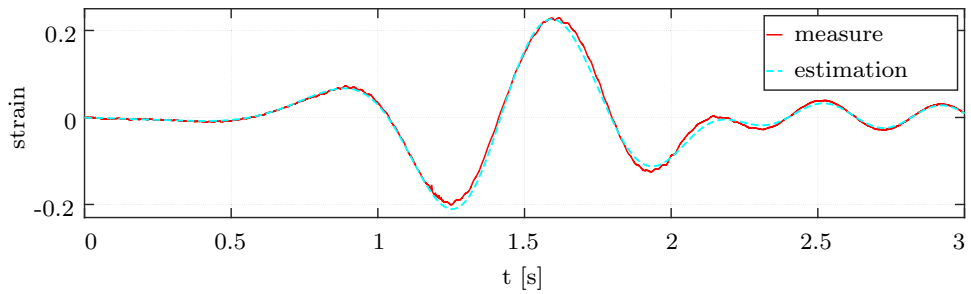

(b) Strain of the long flexible link

Fig. 7 Measurement and estimation results of the lambda robot for a nonlinear trajectory

Table 1 Frequency comparison of the links of the two models

Model	Link	f_1	f_2	f_3	f_4	f_5	f_6
Model-1	Long link	2.49	20.42	37.48	71.18	110.7	145.8
	Short link	–	–	–	–	–	–
Model-2	Long link	2.46	20.30	37.23	70.81	110.4	145.5
	Short link	13.99	–	–	–	–	–

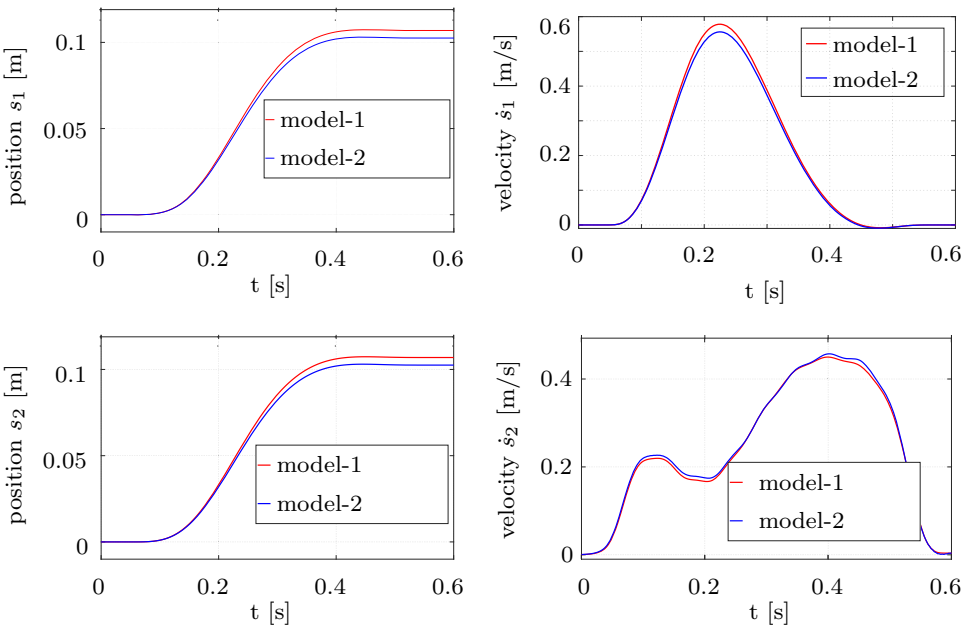

Fig. 8 Feedforward control part results for the two actuators based on the two models

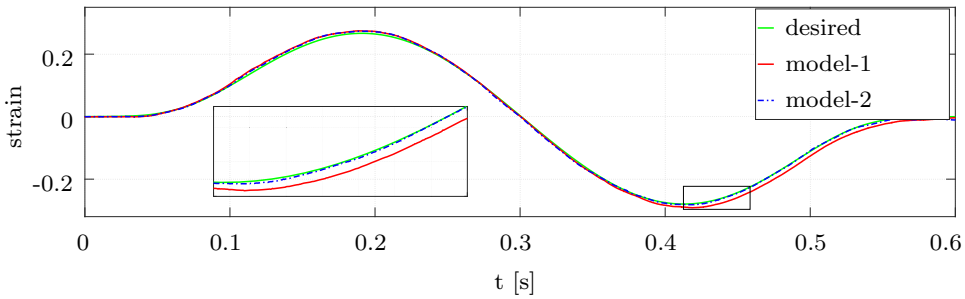

(a) Comparing the strain of the two models

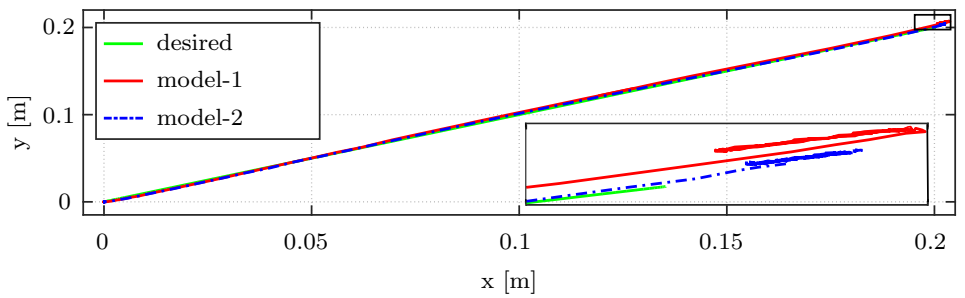

(b) Comparing the end-effector position of the two models

Fig. 9 Comparing the experimental results of the two models for tracking a line trajectory (maximum velocity of end-effector is equal to 1.2374 m/s)

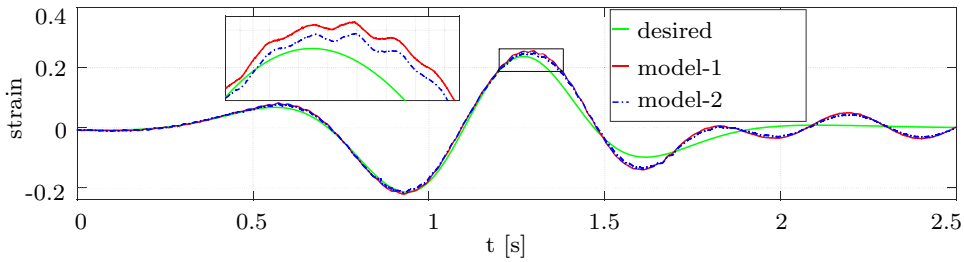

(a) Comparing the strain measurements and desired

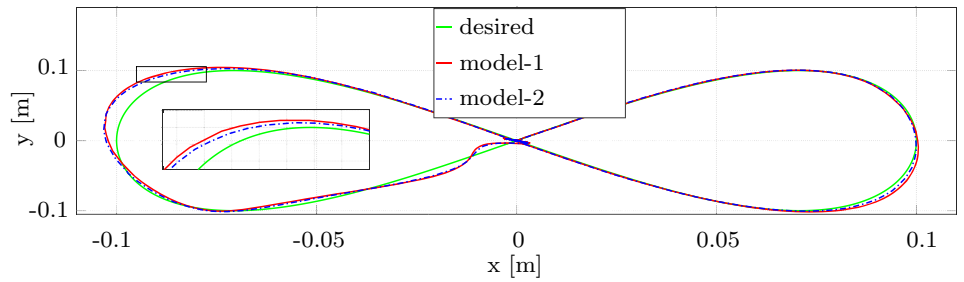

(b) Comparing the end-effector position

Fig. 10 Comparing the experimental results of the two models for tracking a nonlinear trajectory (maximum velocity of end-effector is equal to 1.0245 m/s)

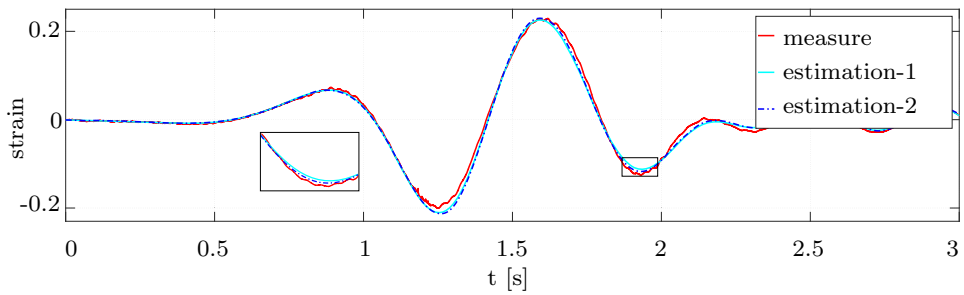

(a) Strain estimation by the two observers for a nonlinear trajectory

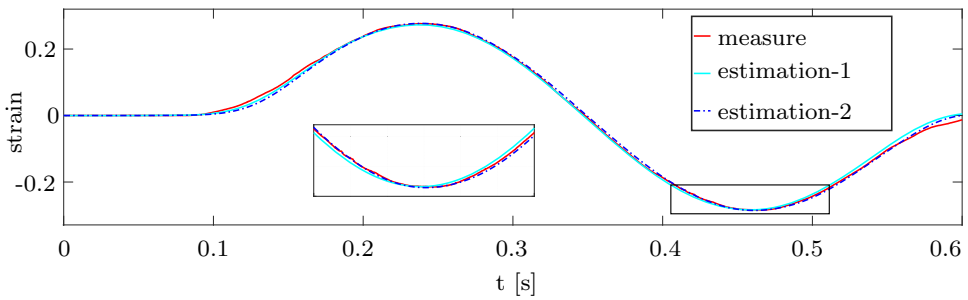

(b) Strain estimation by the two observers for a linear trajectory

Fig. 11 Comparing the strain estimation of the long link by the observers for linear and nonlinear trajectories

1. Also, the first eigen frequency of the short link is about 14 Hz that is not neglectable and so the short link must also be modeled elastic. Therefore, this flexibility is also taken into account in model-2. Thus, there are two improvements of model-2 compared to model-1: improved system parameters and considered the flexibility of the short link.

Again the two-point boundary value problem is solved to find the inverse dynamics solution for the actuators for the model-2 in Sect. 5.1. The feedforward control part allows the position and velocity of the prismatic joints for two models to track a line trajectory as compared in Fig. 8. When a system has higher flexibility and deformation, it needs smaller movements of the actuators to reach the desired position at the end-effector. This is shown in Fig. 8 that the feedforward part results are smaller in model-2 than for model-1.

Next, the feedforward controllers based on the model-1 and the model-2 are implemented on the lambda robot. The experimental results for the two models are shown in Figs. 9

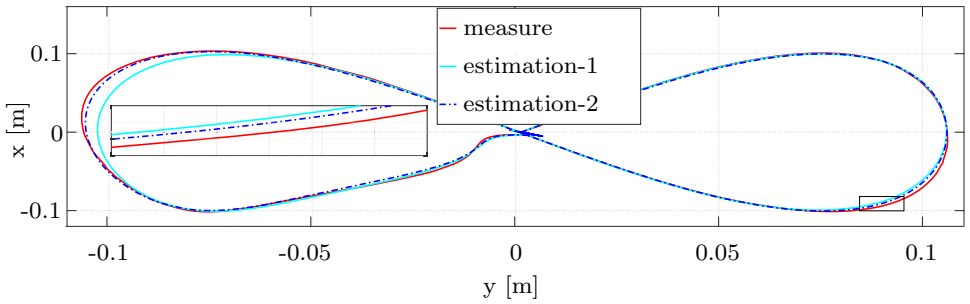

(a) End-effector position estimation by the two observers for a nonlinear trajectory

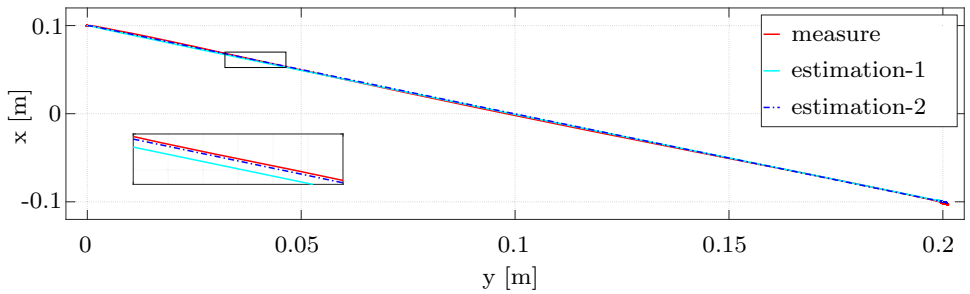

(b) End-effector position estimation by the two observers for a linear trajectory

Fig. 12 Comparing the end-effector estimated positions by the two observers for linear and nonlinear trajectories

and 10 for a linear and a nonlinear trajectory. The strain gauge measurement of two controllers for a linear trajectory is shown in Fig. 9a.

The long link based on the improved model follows well the desired deformation trajectory and this result shows the influence of the model improvement. Also, the end-effector position based on model-2 is closer to the desired trajectory than for model-1. Furthermore, there are smaller oscillation amplitudes and trajectory tracking errors at the end-effector during trajectory tracking.

Comparing the experimental results of the two models shows that the maximum tracking errors and oscillation amplitudes are reduced about 55% and 66.7%, respectively, for a line trajectory. The improved system parameters have the highest effect of about 72% on the improved results and the considered flexibility of the short link has about 28% effect.

The experimental results of tracking a nonlinear trajectory show the improvement clearly in Fig. 10b. For an eight shape trajectory, the end-effector tracks the trajectory at the corner closer to the desired trajectory using the feedforward controller based on model-2. Comparing the results of the two models for an eight shape trajectory also shows that the maximum tracking error and the oscillation amplitude are reduced about 36% and 39%, respectively.

It shall be mentioned that reaching an even smaller error and smaller oscillation amplitude using a feedforward controller is not possible. In order to reduce the tracking error, a feedback controller based the elastic and rigid coordinates is required. For this, the design of a nonlinear observer based on model-2 is needed. Since the estimation using an observer depends on the accuracy of the model, the further estimated states will be more accurate.

6.3 States and end-effector estimation

The designed observer based on model-2 is implemented on the lambda robot for a linear and a nonlinear trajectory tracking. The results of the observer based on the model-1 and the observer based on the model-2 are named estimation-1 and estimation-2, respectively.

The experiment results of observers are shown in Figs. 11 and 12. The deformation of the long link for the two observers and measurements of the strain gauge are compared in Fig. 11. Comparing the estimated deformations shows that the estimation for both observers is close to measurements while comparing the end-effector estimated position in online processing shows just the new observer results (estimation-2) are closer to the camera measurements. These are shown in Fig. 12 for a linear and a nonlinear trajectory.

Measurement results demonstrate the accuracy of the proposed nonlinear observer based on the improved model. The updated nonlinear high gain observer estimates the end-effector position with just about 1 millimeter error for a linear and about 1.5 millimeter error for a nonlinear trajectory.

Conclusions

In this contribution, a nonlinear high gain observer was designed and experimentally applied to a very flexible multibody system. The nonlinear observer uses the position and the velocity of the prismatic joints and only the deformation of the long flexible link. The stability and the convergence of the dynamics error of the estimated states based on the Lyapunov candidate function was shown. The designed observer was used to improve the model of the very flexible multibody system successfully.

Then, the experimental results showed that the measurements are closer to the desired trajectory using the improved model. Furthermore, the tracking error and the oscillation amplitude were drastically decreased for tracking linear and nonlinear trajectories. Also, the designed observer based on the improved model estimated the states and end-effector positions with high accuracy in real-time. This was verified by using an offline validation of image processing and online measurements of strain gauge. The designed observer will be used to design a nonlinear feedback controller based on the estimated states to increase the end-effector trajectory tracking accuracy.

Acknowledgements This research was partially supported by the German Research Foundation, within the Cluster of Excellence in Simulation Technology SimTech at the University of Stuttgart. The authors appreciate these discussions.

References

1. Dwivedy SK, Eberhard P (2006) Dynamic analysis of flexible manipulators, a literature review. Mechanism and Machine Theory 41(7):749–777
2. Aarts RGKM, Jonker JB (2002) Dynamic simulation of planar flexible link manipulators using adaptive modal integration. Multibody Syst Dyn 1(7):31–50
3. Tzafestas S, Kotsis M, Pimenides T (2002) Observer-based optimal control of flexible Stewart parallel robots. J Intell Robot Syst 34(4):489–503
4. Qiao S (2002) Control of flexible-link multiple manipulators. Trans ASME J Dyn Syst Meas Control 124(1):67–75
5. Seifried R, Burkhardt M, Held A (2011) Trajectory control of flexible manipulators using model inversion. In: Proceedings of the ECCOMAS thematic conference on multibody dynamics, Brussels, Belgium
6. Briot S, Khalil W (2014) Recursive and symbolic calculation of the elastodynamic model of flexible parallel robots. Int J Robot Res 33(3):469–483
7. Abe A (2009) Trajectory planning for residual vibration suppression of a two-link rigid–flexible manipulator considering large deformation. Mech Mach Theory 44(9):1627–1639
8. Raff T, Allgöwer F (2007) An impulsive observer that estimates the exact state of a linear continuous-time system in predetermined finite time. In: Proceedings of the mediterranean conference on control and automation, Athens, Greece
9. Natal GS, Chemori A, Pierrot F, Company O (2010) An experimental comparison of state observers for the control of a parallel manipulator without velocity measurements. In Proceedings of the international conference on intelligent robots and systems, IROS/IEEE/RSJ, Taipei, Taiwan
10. Khalil HK, Praly L (2014) High-gain observers in nonlinear feedback control. Int J Robust Nonlinear Control 24(6):993–1015
11. Astolfi D, Marconi L, Praly L, Teel A (2016) Sensitivity to high-frequency measurement noise of nonlinear high-gain observers. IFAC PapersOnLine 49(16):862–866
12. Ahrens JH, Khalil HK (2009) High-gain observers in the presence of measurement noise: a switched-gain approach. Automatica 45(4):936–943
13. Chalhoub NG, Kfoury G, Bazzi B (2006) Design of robust controllers and a nonlinear observer for the control of a single-link flexible robotic manipulator. J Sound Vib 291(1):437–461
14. Nguyen TD, Egeland O (2008) Infinite dimensional observer for a flexible robot arm with a tip load. Asian J Control 10(4):456–461
15. Ju J, Li W, Wang Y, Fan M, Yang X (2009) Two-time scale virtual sensor design for vibration observation of a translational flexible-link manipulator based on singular perturbation and differential games. Sensors 16(11):1804–1818
16. Morlock M, Schröck C, Burkhardt M, Seifried R (July 2017) Nonlinear state estimation for trajectory tracking of a flexible parallel manipulator. In: IFAC world congress, Toulouse, France
17. Benosman M, Le Vey G (2004) Control of flexible manipulators: a survey. Robotica 22(5):533–545
18. Kiang CT, Spowage A, Yoong CK (2015) Review of control and sensor system of flexible manipulator. J Intell Robot Syst 77(1):187–213
19. Bakhti M, Bououlidi Idrissi B (2015) Active vibration control of a flexible manipulator using model predictive control and Kalman optimal filtering. Int J Eng Sci Technol IJEST 5(1):165–177
20. Gu M, Piedbuf J-C (2003) A flexible-arm as manipulator position and force detection unit. Control Eng Pract 11(12):1433–1448
21. Dogan M, Morgül Ö (2010) On the control of two-link flexible robot arm with nonuniform cross section. J Vib Control 16(5):619–646
22. Burkhardt M, Holzwarth P, Seifried R (2013) Inversion based trajectory tracking control for a parallel kinematic manipulator with flexible links. In: Proceedings of the 11th international conference on vibration problems, Lisbon, Portugal
23. Burkhardt M, Seifried R, Eberhard P (2014) Experimental studies of control concepts for a parallel manipulator with flexible links. In: Proceedings of the 3rd joint international conference on multibody system dynamics and the 7th Asian conference on multibody dynamics, Lisbon, Portugal
24. Fehr J, Grunert D, Holzwarth P, Fröhlich B, Walker N, Eberhard P (2018) Morembs—a model order reduction package for elastic multibody systems and beyond. In: KoMSO challenge workshop on reduced-order modeling for simulation and optimization. https://doi.org/10.1007/978-3-319-75319-5_7
25. Kurz T, Burkhardt M, Eberhard P (2011) Systems with constraint equations in the symbolic multibody simulation software Neweul-M^2. In: Proceedings of the ECCOMAS thematic conference on multibody dynamics, Brussels, Belgium
26. Wallrapp O (1994) Standardization of flexible body modeling in multibody system codes, part i: definition of standard input data. Mech Struct Mach 22(3):283–304
27. Primbs J (1996) Survey of nonlinear observer design techniques. Penn State Notes 1(1):1–18
28. Khalil HK (2008) High-gain observers in nonlinear feedback control. In: Proceedings of the international conference on control, automation and systems, ICCAS, Seoul, Korea
29. Blajer W, Kolodziejczyk K (2004) A geometric approach to solving problems of control constrains: theory and a DAE framework. Multibody Syst Dyn 11(4):343–364